IMCC Journal of Science
2022, 2, 31-42
https://myjournal.imcc.edu.ph/

Development of an X-ray Shielding Material Based on Eggshells and Crab Shells

Mark Alipio [1,*], Emerson Paul Somontan [1], Prince Eroll Reyes [1], Grace Meroflor Lantajo [2]
[1] Iligan Medical Center College, Iligan City, Lanao del Norte, Philippines; eds35732@imcc.edu.ph (E.P.S.); pvr35832@imcc.edu.ph (P.E.R.)
[2] University of Southeastern Philippines, Davao City, Davao del Sur, Philippines; gmlantajo@gmail.com (G.M.L.)
* Correspondence: markmalipio@gmail.com

ABSTRACT
Despite the significant role of X-ray radiation in medicine and industry, its excessive use poses a variety of harmful effects ranging from hair loss to death. These effects have been reduced using commercially available lead (Pb) shields. However, Pb-shielding materials are expensive, less durable, highly toxic, very heavy, and uncomfortable to wear for both X-ray machine operators and patients. Eggshells and crab shells are waste materials that are potentially capable of shielding X-rays. In this study, the shielding efficacy, mass, and durability of eggshell and crab shell samples were characterized using diagnostic X-ray energies from 30 to 150 kV and were compared to the standard Pb shield. Linear attenuation coefficient (μ) and radiation protection efficiency (RPE) were used to measure the shielding efficacy of the samples. The required thickness necessary to provide 90%, 95%, and 99% protection at 150 kV energy was also calculated. Across the diagnostic X-ray energy range, the brown eggshell-crab shell-silicone rubber (BE-C-SR) sample obtained the highest μ and RPE. This sample had the least thickness required to provide 90%, 95%, and 99% protection at 150 kV energy. The compressive strength and flex resistance values of BE-C-SR were closer to those of the standard Pb shield. In conclusion, BE-C-SR could be a good alternative to Pb-shielding materials owing to its lower cost, smaller mass, and comparable shielding efficacy and durability.

KEYWORDS: eggshells; crab shells; Lead; X-ray shielding

ARTICLE INFO: Received: 21 February 2021; Accepted: 06 October 2022; Volume: 02; Issue: 02; Type: Original Article

1. Introduction

X-ray radiation plays a pivotal role in medical diagnosis and therapeutics, material science, safety, and industry, among others. However, excessive X-ray radiation is harmful to humans and results in skin burns, infertility, loss of hair, cataracts, increased incidence of cancer, and worst, death. Therefore, shielding devices have been developed to protect the public, especially the patients and occupational workers from the harmful effects of radiation [1]. According to the International Commission on Radiological Protection, diagnostic radiology facilities must be

equipped with shielding devices [2]. Lead-shielding materials are commonly used because they provide the greatest protection against X-rays. However, these shielding materials are costly, very heavy, and uncomfortable to wear for a longer examination time, which could pose serious orthopedic problems.

In addition to cost and weight, the toxicity of Pb is a significant concern, and its disposal is associated with some environmental hazards [3]. Moreover, Pb aprons, which are composed of layered thin Pb sheets, have common cracking problems in practice due to bending and incorrect hanging after use [4].

Considering the properties of Pb, there is a need to find an alternative. Clay-white cement mixture, silica-based commercial glasses, Ball clay and Kaolin, coated textiles, mortars made with cement, sand, and eggshells, polymer nanocomposites, and fabrics coated with Tungsten and Barium sulfate additives were found to shield radiation [5-11]. However, these materials have limited availability in the Philippines. In addition, experimental setups of these studies failed to compare the linear attenuation coefficients of the experimental and standard Pb shields. None also formulated a device that shields X-rays in the diagnostic range (30-150 kV), the range in which all of the medical imaging procedures involving X-rays are conducted. Other parameters such as weight, compressive strength, and flexural strength that are essential to increasing the durability and user acceptability of the shield were not tested. The samples used in the previous studies have economic value, thus may compromise the profit of the manufacturing firms. In general, there is still a need to find practical alternatives to Pb.

Globally, much effort has been made to convert waste material into useable products. Majority of the waste products are food wastes such as chicken eggshells and crab shells. Chicken eggshells are commercial food processing and manufacturing by-products that are primarily composed of Calcium carbonate ($CaCO_3$) [12]. Similarly, crab shells mainly contain $CaCO_3$ and inorganic minerals. It was reported that the high number of $CaCO_3$ particles deposited within the chitin-protein matrix of crab shells allowed the material to resist high tensile stress, strong forces, and high temperature [13]. Another study showed that the trace amount of Magnesium atoms in $CaCO_3$ crystal cause nonuniformities in the structure of the crystal, thus increasing the stiffness of the mineral, which in turn hardened the crab shells [14]. The stiffness, molecular complexity, and tensile strength parameters are related to the effective atomic number and mass density. Meanwhile, specific gravity, eggshell weight, and eggshell surface area were found to be high in eggshells [15,16]. These parameters are directly related to the linear attenuation coefficient, the primary factor that should be considered in the construction of ideal shielding material [17].

Few studies have been carried out concerning the shielding effectiveness of eggshells against radiation. In a previous study, eggshells had under 10% transmittance of Ultraviolet (UV) radiation [18]. In the same study, the shielding efficacy was 43.5% higher for white eggshells and 57.1% higher for brown eggshells than nylon with Titanium dioxide particles. On the other hand, eggshells were used as an additive to increase the radiation absorption property of mortars [9,19]. The addition of eggshells improved the linear attenuation coefficient of mortars from 1.49 cm^{-1} to 3.66 cm^{-1} at 26.1 keV gamma-ray energy. The result of this study also revealed that an increase in the eggshell powder additive ratio increased the linear attenuation coefficient of the

mortars. However, the former study tested eggshells' efficacy as shielding against UV radiation, a type of radiation that has lower frequency and energy compared to X-rays. The latter study utilized cement as the binding material for eggshells which is very heavy. Thus, it may hinder specific movements and pose uneasiness for the patient and operators who seek protection. In terms of durability to cracking, flexibility after curing, viscosity, resilience, and strength, Silicone Rubber (SR) has been superior compared to other binding agents for shielding composites [8]. This coating agent can excellently hold heavy powders with high density in dispersed form. The flex resistance test results revealed that 40% Silicone Rubber and 60% additive material could not crack up to 250 flex cycle counts [11]. This mix proportion was also utilized by a previous study and yielded similar shielding efficacy [8].

To address the issues of radiation effects, cost, weight, toxicity and disposal of Pb shields, and solid waste management, the present study aims to develop an alternative X-ray shielding material based on eggshells and crab shells for X-ray machine operators and patients. Specifically, it seeks to determine the shielding efficacy measured by linear attenuation coefficient and radiation protection efficiency of chicken eggshells and crab shells relative to standard Pb shield, to assess the thickness of chicken eggshells, crab shells, and standard Pb shield required to provide 90%, 95%, and 99% radiation protection efficiency values, and to determine and compare the mass, compressive strengths, and flex resistance as measured by flex count cycles of chicken eggshells, crab shells, and standard Pb shield.

2. Materials and Methods

2.1 Collection and Preparation of Chicken Eggshells and Crab Shells and Elemental Analysis

Brown and white eggshells (BE, WE) were collected from a commercial farm in Iligan City, Philippines. The crab shells (C) were taken from commercial food entities in the same location. After retrieval, the shells were washed with distilled water and air-dried for five days at a temperature range of 25-30 ^{0}C. These were then ground into powder using a grinding pulverizer machine. After grinding, these were filtered through a 75-micron sieve. An X-ray fluorescence (XRF) spectrometer was used to determine the elemental concentrations of the shells. The compositions are listed in Table 1.

2.2 Preparation of Shields

The shields were prepared in accordance with fluoropolymer application standards which were used in the previous studies on the shielding effectiveness of fabrics coated with Tungsten and Barium sulfate additives and coated textiles [8,11,20]. A liquid silicone rubber (J. Spencer Technologies, Philippines) was used as the commercial binding agent. The sieved eggshells and crab shells were mixed with SR for 1 hour using the weight ratio of 60% additive and 40% SR. To avoid air bubbling, the shell-SR mixture was degassed by vacuuming for 30 minutes. After degassing, this underwent curing for 15 minutes at a temperature of 110 ^{0}C to ensure hardening of the

Table 1. Elemental composition of samples.

Elements	Concentration (%)		
	Brown Eggshell	White Eggshell	Crab Shell
Calcium	94.29	90.11	97.10
Phosphorus	2.22	1.11	1.55
Magnesium	1.90	1.10	1.01
Others	1.59	7.68	0.34

Table 2. Sample codes and mix proportions.

Sample Code	Brown Eggshell (%)	White Eggshell (%)	Crab Shell (%)	SR (%)	Pb (%)
SR	0	0	0	100	0
WE-SR	0	60	0	40	0
BE-SR	60	0	0	40	0
C-SR	0	0	60	40	0
WE-C-SR	0	30	30	40	0
BE-C-SR	30	0	30	40	0
Pb	0	0	0	0	100

mixture. A laboratory knife machine was used to create a shield with 300 mm x 300 mm x 0.5 mm dimensions. The experimental shields were then labeled according to the type and color of the shell used. Pb shield and SR with the same measurements were prepared and used as the positive and negative control. The shield sample codes, the materials, and the mixing ratios are given in Table 2.

2.3 Determination of Shielding Efficacy

The radiation shielding efficacy of the samples was measured at 30, 90, and 150 kV tube voltages in accordance with the medical application standards [21]. The analysis was undertaken at the X-ray laboratory of Iligan Medical Center College, Iligan City, Philippines. The following radiographic equipment were prepared: diagnostic X-ray machine (General Electric, USA), radiographic caliper, and Geiger-Mueller (GM) detector.

The experimental shield was placed between the detector and the X-ray source, at a very close position to the GM detector. The distance between the X-ray tube and the GM detector was set at 100 cm, and the X-ray beam was collimated according to the size of the shields (300 mm x 300 mm). Using the radiographic technique of 5.2 milliampere-seconds, a first exposure was taken at 30 kV tube voltage. Each shield was exposed three times using the same tube voltage, and the average value was considered. Another series of exposures was employed at 90 kV and 150 kV tube voltages to capture the diagnostic range of X-rays [1]. The schematic representation of the analysis is given in Figure 1.

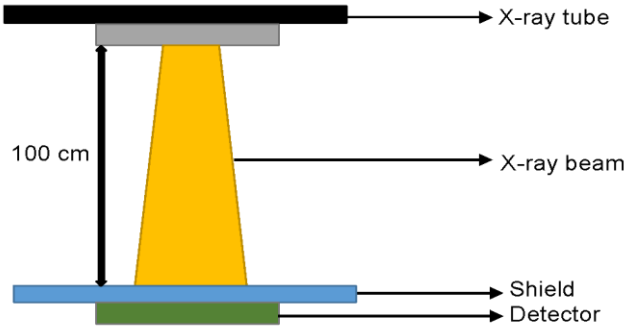

Figure 1. Schematic diagram of the measurement set-up.

A total of 63 radiographic exposures (3 replicates per shield x 7 shields x 3 tube voltages) were analyzed in terms of the intensity of X-rays that pass through a shield using the readings of GM detector. From the intensity readings of the GM detector, the linear attenuation coefficient of each shield was calculated using the formula:

$$\mu = -\frac{ln\left(\frac{I}{I_0}\right)}{t} \quad (1)$$

Where μ is the linear attenuation coefficient, I is the intensity of X-ray radiation after interaction with shielding material, I_o is the initial intensity, and t is the thickness of shielding material in centimeters.

Using the same intensity readings of the GM detector, the radiation protection efficiency of each shield was computed using the following formula:

$$RPE = \left(1 - \frac{I}{I_0}\right) * 100 \quad (2)$$

Where RPE is the radiation protection efficiency, I is the intensity of X-ray radiation after interaction with shielding material, and I_o is the initial intensity.

Readings of the intensity of X-ray radiation after interaction with shielding material, initial intensity, and thickness of shielding material were encoded in Microsoft Excel 2016. A code in Excel based on the formula above was used to calculate the linear attenuation coefficient and radiation protection efficiency.

2.4 Determination of Required Thickness for 90%, 95%, and 99% Radiation Protection Efficiency

An RPE of 90%, 95%, and 99% of shield at 150 kV level is required in medical diagnostic applications [8]. The required thickness of the seven shields for 90%, 95%,

and 99% RPE values at 150 kV was calculated using the derived and combined formula of linear attenuation coefficient and RPE:

$$t = -\frac{ln\left(\frac{I}{I_0}\right)}{\mu}$$

$$\frac{I}{I_0} = 1 - RPE$$

$$t = -\frac{ln(1-RPE)}{\mu} \quad (3)$$

2.5 Determination of Mass, Compressive Strength and Flex Resistance of the Shields

The calculated thickness from the derived equation was used to develop shields based on eggshells and crab shells with comparable radiation protection efficiency as that of the standard Pb shield.

The same steps were employed in the formulation of the optimized shields. The shields were developed with 300 mm x 300 mm x *calculated thickness in mm* dimensions. The mass in terms of g of the shields was measured using an electronic balance. Three measurements were taken, and the mean value was calculated.

The compressive strength test was conducted following the ASTM C 109 standards. The samples were tested using Mitutoyo Universal Testing Machine of capacity 1,000 kilonewtons at a loading rate of 0.25 psi per second. The test was conducted in three replicates, and the average compressive strength value measured as psi was considered.

The shields were sent to a mechanical testing laboratory for flex resistance analysis. The test was conducted following ISO 5402-1:2011. A flexometer device was used to hold the two edges of the shields. In each flex cycle, the shields were subjected to severe crumpling motion. The shields were observed until any damage was detected. The flex resistance was measured based on the flex count cycle (fcc) in which the damage is detected.

2.6 Data Analysis

All measurements were done in triplicates. Mean and standard deviation (SD) were used to determine the average linear attenuation coefficient, radiation protection efficiency, mass, psi, and fcc of the shields.

3. Results and Discussion

In this study, the shielding efficacy was carried out by exposing the samples, which are in close contact with a detector, using constant radiographic techniques, namely milliampere-seconds and distance between detector and X-ray tube. Kilovoltage, however, was varied from 30 to 150 to capture the energy range of diagnostic X-rays.

Table 3. Linear attenuation coefficients, μ (cm^{-1}) of the studied samples at the given X-ray energies (n = 3, results depicted as mean ± SD).

Sample Code	30 kV	90 kV	150 kV
SR	0.003 ± 0.011	0.002 ± 0.004	0.000 ± 0.006
WE-SR	0.089 ± 0.010	0.036 ± 0.007	0.002 ± 0.013
BE-SR	0.147 ± 0.006	0.081 ± 0.010	0.015 ± 0.014
C-SR	0.212 ± 0.007	0.123 ± 0.015	0.019 ± 0.003
WE-C-SR	0.230 ± 0.009	0.136 ± 0.007	0.033 ± 0.005
BE-C-SR	0.306 ± 0.013	0.179 ± 0.009	0.045 ± 0.010
Pb	0.573 ± 0.012	0.287 ± 0.014	0.058 ± 0.015

Linear attenuation coefficients, μ (cm^{-1}) of the studied samples, calculated from the intensity readings of the GM detector at the given X-ray energies, are shown in Table 3. The attenuation of X-rays depends on the energy of incident X-ray and the properties of the material through which the X-ray traverses [1]. Therefore, the incident X-ray energy and the atomic number, thickness, and density of the material, affect the attenuation of X-rays [17]. In the study, it can be observed that the calculated μ of all samples decreased with increment of X-ray energy. This is based on the photoelectric effect of X-rays on the material. Increasing X-ray energy means increasing the penetrability of X-rays [1]. This phenomenon tends to increase the number of X-rays transmitted to the studied samples, which decreases the attenuation coefficients.

The thicker the attenuating material, the higher is the attenuation coefficient [1]. In this study, the samples were prepared with the same dimensions. Therefore, thickness did not affect the attenuation coefficients of the samples. It is assumed that the atomic number and density of the material are the remaining factors that explain the attenuation coefficient of the samples. Although the atomic number and density were not measured in the study, it can be inferred that Pb had the highest atomic number and density among the studied samples. This is based on the notion that materials with a high atomic number and high density have high attenuation coefficients [1,17].

Of the experimental samples, BE-C-SR had the highest linear attenuation coefficients across the three X-ray energies. On the other hand, SR had the lowest linear attenuation coefficients. The addition of eggshells to SR increased the attenuation coefficients. This is similar to the previous study, which used eggshells as an additive to increase the radiation absorption property of mortars [9]. The addition of eggshells improved the linear attenuation coefficient of mortars from 1.49 cm^{-1} to 3.66 cm^{-1} at 26.1 keV gamma-ray energy. The result of this prior study also revealed that an increase in the eggshell powder additive ratio increased the linear attenuation coefficient of the mortars. The samples with BE showed a higher linear attenuation coefficient compared to those of their WE counterpart. A possible explanation for this result is that BE could have a higher atomic number and density than WE. Previous studies reported differences in BE and WE in terms of shell thickness, specific gravity, and breaking strength [13,14]. Specific gravity, eggshell weight, and eggshell surface area were statistically higher in BE than WE [15,16]. These three parameters are directly proportional to mass density, one of the factors that should be considered in constructing a shielding material [17].

Table 4. RPE (%) of the studied samples at the given X-ray energies (n = 3, results depicted as mean ± SD).

Sample Code	30 kV	90 kV	150 kV
SR	1.320 ± 0.008	0.823 ± 0.006	0.020 ± 0.008
WE-SR	35.910 ± 0.012	16.530 ± 0.008	0.957 ± 0.010
BE-SR	52.040 ± 0.013	33.210 ± 0.012	6.997 ± 0.012
C-SR	65.310 ± 0.011	45.970 ± 0.010	9.210 ± 0.013
WE-C-SR	68.310 ± 0.014	49.320 ± 0.009	15.320 ± 0.007
BE-C-SR	78.310 ± 0.010	59.210 ± 0.015	20.321 ± 0.010
Pb	94.310 ± 0.016	76.230 ± 0.013	25.230 ± 0.012

Besides, the addition of crab shells to the eggshell-SR mixture demonstrated the highest linear attenuation coefficients. It was reported that the high number of $CaCO_3$ particles deposited within the chitin-protein matrix of crab shells allowed the material to resist high tensile stress, strong forces, and high temperature [22]. Another study showed that the trace amount of Magnesium atoms in $CaCO_3$ crystal causes nonuniformities in the structure of the crystal, thus increasing the stiffness of the mineral, which in turn hardened the crab shells [23]. The stiffness, molecular complexity, and tensile strength parameters are related to the effective atomic number and mass density, two components considered in constructing a shielding material [17].

The RPE was theoretically calculated using the initial intensity and intensity of X-ray radiation after interaction with the studied samples, as provided in Equation (2). This parameter is an essential measure of shielding efficacy as this is the percentage of shielded radiation after passing through a material. Materials with a higher RPE allow a greater number of absorbed or scattered x-rays when controlling for thickness and, thus, could shield radiation better [24,25]. Conversely, materials with lower RPE allow a higher number of transmitted x-rays when controlling for thickness and, thus, have lower shielding efficacy. The RPE of the studied samples is shown in Table 4. Based on the table, the RPEs were reduced with an increment of X-ray energy. Among the experimental samples, BE-C-SR demonstrated the highest RPE across all X-ray energies. The highest RPE was observed at 30 kV in the BE-C-SR sample. Meanwhile, SR showed the lowest RPE across all X-ray energies.

The RPE results imply that among the experimental samples, BE-C-SR showed the highest percentage of X-rays shielded after passing through it. Therefore, this sample had the highest X-ray shielding efficacy. Due to its high density and molecular complexity, which could directly affect the atomic number, more X-rays are shielded with BE-C-SR, especially for the X-rays with low energy compared to the other experimental samples. The probability of X-ray interaction with the BE-C-SR atoms is comparatively high due to the tightly-packed particles inside the sample. Further studies are needed to measure the density and visually describe the molecular structure of the samples to explain this result better.

An RPE of 90%, 95%, and 99% of shield at 150 kV level is required in medical diagnostic applications [8]. The required thickness of the seven samples for 90%, 95%, and 99% RPEs at 150 kV were calculated using the Equation (3). Among the experimental samples, BE-C-SR had the least thickness necessary to provide 90%, 95%, and 99% protection at 150 kV energy. Because BE-C-SR had the highest calculated μ

Table 5. Required thickness (mm) for 90%, 95%, and 99% RPEs at 150 kV (n = 3, results depicted as mean ± SD).

Sample Code	90% RPE	95% RPE	99% RPE
SR	57558.871 ± 0.019	74885.817 ± 0.018	115117.741 ± 0.019
WE-SR	1197.848 ± 0.013	1558.436 ± 0.012	2395.696 ± 0.009
BE-SR	158.715 ± 0.015	206.493 ± 0.015	317.430 ± 0.020
C-SR	119.155 ± 0.017	155.025 ± 0.018	238.311 ± 0.022
WE-C-SR	69.234 ± 0.019	90.075 ± 0.019	138.467 ± 0.019
BE-C-SR	50.681 ± 0.020	65.938 ± 0.010	101.362 ± 0.017
Pb	39.597 ± 0.013	51.517 ± 0.012	79.194 ± 0.019

and RPE, less shielding is required in BE-C-SR to attenuate the same number of X-rays when compared to other samples. This result conforms to Equation (3), demonstrating that the required thickness of a material to achieve the given RPE is inversely related to its μ. Higher μ values require lesser thickness to shield a given number of X-rays.

The required thickness of the samples (Table 5) for 90%, 95%, and 99% RPEs at 150 kV was used to develop new shields. All samples were designed with the following dimensions: 300 mm length x 300 mm width x *calculated thickness in mm* provided in Table 5. With the new dimensions, the mass (g), compressive strength (psi), and flex resistance (fcc) were measured. Compared to Pb, all experimental samples were less massive. Approximately, the mass of all experimental samples was one-half times less than that of Pb. This result may address the concerns of heaviness and discomfort posed by wearing Pb for a longer examination time during a radiographic procedure.

The durability of the samples was measured using the obtained compressive strength and flex resistance values. It can be noted that the addition of eggshells increased the durability of the SR. The addition of crab shells increased even more the durability of the eggshells-CR mixture. Across all X-ray energies, BE-C-SR demonstrated the highest compressive strength and flex resistance among the experimental samples. The compressive strength and flex resistance values of BE-C-SR were closer to the standard Pb shield.

4. Conclusion

BE-C-SR could be a potential candidate as an X-ray shielding material for X-ray machine operators and patients. Across the 30-150 kV range of diagnostic X-rays, this sample obtained the highest μ and highest RPE. The sample had the least thickness necessary to provide 90%, 95%, and 99% protection at 150 kV energy. The compressive strength and flex resistance values of BE-C-SR were closer to those of the standard Pb shield. In conclusion, BE-C-SR might be an alternative X-ray shielding material for commercial and practical utilization owing to its low cost, smaller mass, and comparable shielding efficacy and durability with the standard Pb shield.

Table 6. Mass (g), compressive strength (psi) and flex resistance (fcc) of the shields at 90%, 95%, and 99% RPE (n = 3, results depicted as mean ± SD).

Sample Code	90% RPE			95% RPE			99% RPE		
	Mass	Compressive Strength	Flex Resistance	Mass	Compressive Strength	Flex Resistance	Mass	Compressive Strength	Flex Resistance
SR	9.856 ± 0.012	1.694 ± 0.092	39.021 ± 0.041	16.388 ± 0.093	1.894 ± 0.083	3.749 ± 0.094	2.489 ± 0.012	0.168 ± 0.012	0.037 ± 0.001
WE-SR	329.996 ± 0.092	46.077 ± 0.075	73.186 ± 0.048	358.305 ± 0.049	38.049 ± 0.037	13.725 ± 0.091	119.613 ± 0.123	8.049 ± 0.492	1.794 ± 0.298
BE-SR	545.049 ± 0.016	66.774 ± 0.016	97.333 ± 0.018	800.395 ± 0.048	76.443 ± 0.084	18.349 ± 0.093	902.739 ± 0.942	58.881 ± 0.851	13.540 ± 0.938
C-SR	785.317 ± 0.060	83.801 ± 0.076	105.649 ± 0.017	1220.831 ± 0.028	105.814 ± 0.038	23.816 ± 0.018	1202.447 ± 0.493	77.504 ± 0.309	18.035 ± 0.489
WE-C-SR	852.410 ± 0.081	87.651 ± 0.085	152.221 ± 0.012	1347.763 ± 0.090	113.526 ± 0.013	34.038 ± 0.129	2069.484 ± 0.893	128.921 ± 0.924	31.039 ± 0.693
BE-C-SR	1133.649 ± 0.011	100.482 ± 0.084	251.420 ± 0.021	1778.273 ± 0.039	136.290 ± 0.092	39.272 ± 0.194	2827.052 ± 0.982	171.005 ± 0.359	42.401 ± 0.529
Pb	2126.231 ± 0.098	121.012 ± 0.082	8417.597 ± 0.033	2849.150 ± 0.048	175.467 ± 0.093	44.484 ± 0.178	3618.420 ± 0.394	212.316 ± 0.238	54.270 ± 0.892

Acknowledgment

The authors express their sincere gratitude to Iligan Medical Center College (IMCC) for providing the financial support that made this research possible.

Conflict of Interest Statement

The authors declare no conflict of interest.

Author Contributions: All authors contributed equally to this work and agreed to publish this paper in this journal.

References

1. Bushong, S.C. *Radiologic science for technologists: Physics, biology, and protection,* 10th ed.; Elsevier Health Sciences: Philadelphia, United States, 2016.
2. Annals of the ICRP. Available online: https://doi.org/10.1016/j.icrp.2007.10.003 (accessed on 18 February 2018).
3. Moawad, E.M.; Badawy, N.M.; Manawill, M. Environmental and occupational lead exposure among children in Cairo, Egypt: A community-based cross-sectional study. *Medicine* **2016**, *95*, e2976.
4. Oyar, O.; Kislalioglu, A. How protective are the lead aprons we use against ionizing radiation? *Diagn Interv Radiol* **2012**, *18*, 147-152.
5. Akbulut, S.; Sehhatigdiri, A.; Eroglu, H.; Celik, S. A research on the radiation shielding effects of clay, silica fume and cement samples. *Radiat Phys Chem* **2015**, *117*, 88-92.
6. Yasmin, S.; Rozaila, Z.S.; Khandaker, M.U.; Barua, B.S.; Chowdhury, F.U.; Rashid, M.A.; Bradley, D.A. The radiation shielding offered by the commercial glass installed in Bangladeshi dwellings. *Radiat Eff Defect S* **2018**, *173*, 657-672.
7. Olukotun, S.F.; Gbenu, S.T.; Ibitoye, F.I.; Oladejo, O.F.; Shittu, H.O.; Fasasi, M.K.; Balogun, F.A. Investigation of gamma radiation shielding capability of two clay materials. *Nucl Eng Technol* **2018**, *50*, 957-962.
8. Aral, N.; Nergis, F.; Candan, C. An alternative X-ray shielding material based on coated textiles. *Text Res J* **2015**, *86*, 803-811.
9. Binici, H.; Aksogan, O.; Sevinc, A.H.; Cinpolat, E. Mechanical and radioactivity shielding performances of mortars made with cement, sand and egg shells. *Constr Build Mater* **2015**, *93*, 1145-1150.
10. Nambiar, S.; Osei, E.K.; Yeow, J.T. Polymer nanocomposite-based shielding against diagnostic X-rays. *J Appl Polym Sci* **2013**, *127*, 4939-4946.
11. Aral, N.; Nergis, F.; Candan, C. Investigation of x-ray attenuation and the flex resistance properties of fabrics coated with tungsten and barium sulphate additives. *Tekstil ve Konfeksiyon* **2016**, *26*, 166-171.
12. Stadelman, W.J. *Eggs and egg products*, 2nd ed; John Wiley & Sons: New York, United States, 2000; pp. 593–599.
13. Şekeroglu, A.; Duman, M. Effect of egg shell colour of broiler parent stocks on hatching results, chickens performance, carcass characteristics, internal organ

weights and some stress indicators. *Kafkas Üniversitesi Veteriner Fakültesi Dergisi* **2011**, *17*, 837-842.
14. Potts, P.L.; Washburn, K.W. Shell evaluation of white and brown egg strains by deformation, breaking strength, shell thickness and specific gravity: Relationship to egg characteristics. *Poult Sci* **1974**, *53*, 1123-1128.
15. Joseph, N.S.; Robinson, N.A.; Renema, R.A.; Robinson, F.E. Shell quality and color variation in broiler breeder eggs. *J Appl Poultry Res* **1999**, *8*, 70-74.
16. Soria, M.A.; Bueno, D.J.; Bernigaud, I.I. Comparison of quality parameters in hen's eggs according to egg shell color. *Int J Poult Sci* **2013**, *12*, 224-234.
17. Goel, V. K. *Fundamentals of Physics XI*; McGraw-Hill Education: India, 2007.
18. Fecheyr-Lippens, D.; Nallapaneni, A.; Shawkey, M. Exploring the use of unprocessed waste chicken eggshells for UV-protective applications. *Sustainability* **2017***, 9*, 232.
19. Alipio M.M. Eggshells as alternative shielding material against diagnostic X-rays. *CMU J Sci* **2020**, *23*, 37-43.
20. Ebnesajjad, S.; Khaladkar, P. *Applications in chemical processing industries,* 2nd ed.; William Andrew: New York, United States, 2004.
21. Bushong, S.C. *Workbook for radiologic science for technologists: Physics, biology, and protection,* 5th ed.; Elsevier Health Sciences: Philadelphia, United States, 2016.
22. Gbenebor O.P.; Adeosun S.O.; Lawal G.I.; Jun S. Role of CaCO3 in the physicochemical properties of crustacean-sourced structural polysaccharides. *Mater Chem Phys* **2016**, *184*, 203-209.
23. Mincea M.; Negrulescu A.; Ostafe V. Preparation, modification, and applications of chitin nanowhiskers: A review. *Rev Adv Mater Sci* **2012**, *30*, 225-242.
24. Huda, W. *Review of radiologic physics*; Lippincott Williams & Wilkins: Philadelphia, United States, 2010.
25. Fosbinder, R.; Orth, D. *Essentials of radiologic science*, 2nd ed.; Lippincott Williams & Wilkins: Philadelphia, United States, 2011.

Publisher's Note: IMCC stays neutral with regard to jurisdictional claims in published maps and institutional affiliations.